Formation of casein micelles simulating human milk casein composition from bovine caseins : Micellar structure and in vitro infant gastrointestinal digestion

Food Hydrocolloids

Yang, Tingting; Liu, Dasong; Tang, Jun; Tao, Xiumei; Zhang, Jielong et al

https://doi.org/10.1016/j.foodhyd.2023.109610

Food Hydrocolloids 149 (2024) 109610

Contents lists available at ScienceDirect

Food Hydrocolloids

journal homepage: www.elsevier.com/locate/foodhyd

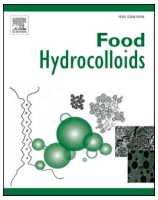

Formation of casein micelles simulating human milk casein composition from bovine caseins: Micellar structure and *in vitro* infant gastrointestinal digestion

Tingting Yang [a,b], Dasong Liu [a,b,*], Jun Tang [a,b], Xiumei Tao [a,b], Jielong Zhang [a,b], Xiaoming Liu [a,b], Thom Huppertz [c,d], Joe M. Regenstein [e], Peng Zhou [a,b]

[a] State Key Laboratory of Food Science and Resources, Jiangnan University, Wuxi, Jiangsu Province 214122, China
[b] School of Food Science and Technology, Jiangnan University, Wuxi, Jiangsu Province, 214122, China
[c] Food Quality and Design Group, Wageningen University & Research, Wageningen, the Netherlands
[d] FrieslandCampina, Amersfoort, the Netherlands
[e] Department of Food Science, Cornell University, Ithaca, NY 14853-7201, USA

ARTICLE INFO

Keywords:
Bovine casein
Human casein
Milk micelles
Infant gastrointestinal digestion
Infant formula

ABSTRACT

Bovine casein micelles in infant formula differ from human micelles in composition, structure and digestion. Preparation conditions, micellar structure and *in vitro* gastrointestinal digestion under infant of casein micelles formed from bovine caseins but simulating human micelles were investigated. Bovine caseins were fractionated and formulated based on the composition of human caseins, i.e., at a ratio of 68:20:12 for β-, κ- and α_{s1}-caseins. Citrate (Cit), calcium (Ca), and inorganic phosphate (Pi) were added into casein dispersions (0.4% caseins, w/v) to obtain casein micelles. Optical absorbances showed that the optimal conditions of formation were mineral addition in the order of Cit → Ca → Pi over three cycles and final concentrations of 2.1–2.8 mM Cit, 6.1–7.1 mM Ca and 1.5–3.0 mM Pi. For micelles formed using 2.3 mM Cit, 7.1 mM Ca, and 2.8 mM Pi (the average concentrations in human milk), the particle size, micellar hydration, internal structure and morphology were similar to those of human micelles, while the percentage of serum caseins was lower and the molar ratio of Ca:casein was higher. During the gastrointestinal digestion, the gastric flocs, free amino groups and molecular weight distribution of peptides were close to those of human micelles, with casein degradation rate being lower, while the flocs were smaller and the free amino groups and casein degradation rate were higher compared to bovine micelles. These results suggested a potential to form micelles with composition, structure and digestion close to human micelles for use in infant formula.

1. Introduction

In most infant formulae, casein micelles are a major protein source. These are derived mainly from bovine milk. Bovine casein micelles differ from human casein micelles in both composition and structure. Bovine micelles contain α_{s1}-, α_{s2}-, β- and κ-caseins at a ratio of ~4:1:3.5:1.5, while human micelles contain α_{s1}-, β- and κ-caseins with a ratio of ~12:68:20, with no α_{s2}-casein detected (Meng, Uniacke-Lowe, Ryan, & Kelly, 2021). Bovine casein micelles are more mineralized than human micelles, and the molar ratios of calcium to caseins for bovine and human micelles are about 18–19 and 7–9, respectively (Huppertz & Timmer, 2020). The diameter of bovine micelles is ~150 nm, which is larger than that of human micelles (~70 nm) (Meng et al., 2021). Bovine micelles are also denser, and the micellar hydration for bovine and human micelles is about 2.3 and 3.4 g water/g casein, respectively (Yang, Liu, & Zhou, 2022). These differences between bovine and human micelles could lead to differences in digestibility, absorption, allergenicity and bio-functionality, which might cause problems such as insufficient protein utilization and gastrointestinal disorders in formula-fed infants, thus affecting their growth and development (Berton et al., 2012; Roy, Ye, Moughan, & Singh, 2020).

Previously, caseins have been formulated to partially simulate human casein composition, i.e., mainly the proportion of β-casein. Li-Chan and Nakai (1988) reported that by selective coagulation of

* Corresponding author. State Key Laboratory of Food Science and Resources, Jiangnan University, Wuxi, Jiangsu Province 214122, China.
E-mail address: liudasong68@163.com (D. Liu).

https://doi.org/10.1016/j.foodhyd.2023.109610
Received 5 August 2023; Received in revised form 15 November 2023; Accepted 29 November 2023
Available online 4 December 2023

bovine acid caseins with rennin, the ratio of β- to α_{s1}-caseins increased from 0.7 to 3.0, resulting in looser coagula and faster casein degradation during an *in vitro* infant gastric digestion. Huang, Zhang, Lan, and Zhou (2022) reported that by adding β-casein to skim milk, formulated caseins systems containing 66% β-caseins were obtained for an infant formula, which showed looser gastric coagula and faster casein degradation during *in vitro* digestion compared to that formulated with skim milk alone. Zhang et al. (2022) also reported that by mixing β-casein with κ-casein concentrate, a formulated casein composition with β- and κ-caseins with a ratio of 68:20 was obtained for an infant formula, which showed a weakened coagulation behavior and a faster protein hydrolysis compared to that formulated with micellar casein concentrate alone. Currently, there is still limited information regarding the formulation of bovine caseins to best simulate human casein composition, i.e., the ratios of other caseins still differ from human caseins after increasing β-casein.

Casein micelles have also been formed to simulate the native casein micelle structures. Hemar, Xu, Wu, and Ashokkumar (2020) reported that formed micelles with mineralization (molar ratio of calcium to caseins: 19:1), particle size (200 nm) and morphology similar to bovine micelles were obtained by sequentially titrating 10 mM citrate (Cit), 30 mM calcium (Ca) and 22 mM inorganic phosphate (Pi) into a 2.5% (w/w) sodium caseinate solution. The concentrations of these minerals and caseins were almost the same as native bovine micelles. Huppertz et al. (2017) reported that formed micelles with mineralization and a particle size similar to bovine micelles were obtained using 2.5% sodium caseinate, 30 mM Ca, 5 mM magnesium (Mg) and 20 mM Pi. Sood, Lekic, Jhawar, Farrell, and Slattery (2006) reported the formation of micelles using 0.3% formulated bovine caseins with only κ- and β-caseins with a ratio of 1:3, 5–10 mM Ca and 4–8 mM Pi, thus establishing conditions closer to human milk. There is still limited information about the formation of bovine micelles to simulate human casein micelle structures similar to human milk in terms of casein and mineral composition. Even less is known about the gastrointestinal digestion behavior of such formed human-like micelles.

Casein micelles are compact nanocarriers of proteins and minerals, which are otherwise too high in concentrations to be free and stable in many dairy streams, for the growing neonates (Zou et al., 2022). These unique micellar assemblies also have vital roles in regulating nutrients flow into neonatal intestine via coagulation in stomach, further suggesting the necessity of forming micelles simulating human micelles to specifically satisfy the needs of neonates (Zhang et al., 2022). The structures of micelles are greatly affected by *in vitro* formation conditions such as mineral compositions and addition approaches, which hence should be cautiously controlled to obtain micelles similar to human micelles before application (Huppertz et al., 2020). The formed micelles, after concentration e.g. by nanofiltration, could be potentially used to produce infant formula with reduced allergenicity and improved digestibility.

Therefore, the objective of this study was to form casein micelles to simulating human caseins and their mineral compositions. The microstructures and *in vitro* infant gastrointestinal digestibility of the formed casein micelles were studied with a view towards preparing bovine-base infant formula that would be closer to human milk.

2. Methods and materials

2.1. Materials

Fresh bovine milk was purchased from Tianzi Dairy Co., Ltd. (Wuxi, China). Fresh human milk was obtained from 10 healthy donors between 2 and 9 months postpartum, with approval from the Medical Ethics Committee of Jiangnan University (certificate number JNU20210618IRB01). Bovine and human milk were skimmed at 3000×*g* for 30 min at 25 °C using an Avanti J-E centrifuge (Beckman Coulter, Inc., Indianapolis, IN, USA). The bovine and human skim milk were ultracentrifuged at 150,000×*g* for 1 h using an Optima L-100XP ultracentrifuge (Beckman Coulter). The ultracentrifugal supernatant was ultrafiltered at 2500×*g* for 1 h using a Vivaspin 6 concentrator with a nominal 10 kDa molecular weight cut-off (Sartorius Stedim Biotech GmbH, Goettingen, Germany). The ultracentrifugally sedimented casein micelles were reconstituted in the corresponding ultrafiltrate to obtain bovine and human casein micelle dispersions with a casein concentration of 0.4%, w/v, similar to that of human milk (Hailu et al., 2016). Porcine pepsin (3880 U/mg), porcine pancreatin (7.4 U trypsin/mg), porcine bile, pepstatin A, Pefabloc SC, p-toluene-sulfonyl-L-arginine methyl ester (TAME), fluorescein isothiocyanate isomer I, cytochrome C (12,384 Da), aprotinin (6500 Da), bacitracin (1422 Da), Gly-Gly-Arg-Try (451 Da), Gly-Gly-Gly (189 Da) and *o*-phthaldialdehyde (OPA) were obtained from Sigma-Aldrich Co. (St. Louis, MO, USA). All chemicals used were at least of analytical grade.

2.2. Fractionation and formulation of caseins

The flowchart for the fractionation of bovine caseins was shown in Fig. S1. First, HCl (2 M) was added dropwise to bovine skim milk with magnetic stirring to pH 4.6, and the acidified sample was centrifuged at 10,000×*g* for 15 min to precipitate bovine caseins, which were reconstituted in ultrapure water (Heal Force Water Purification System, Canrex Analytic Instrument Co., Ltd., Shanghai, China) to obtain a 2.5% (w/v) casein dispersion. NaOH (2 M) was subsequently added dropwise under magnetic stirring to increase the pH of the casein dispersion to pH 11, after which 2 M $CaCl_2$ was added to a final concentration of 65 mM Ca, followed by pH adjustment to pH 7.0 with 2 M HCl, and centrifugation at 10,000×*g* for 15 min. The pH of the supernatant was adjusted to 3.8 with 6 M HCl and centrifuged at 10,000×*g* for 15 min to obtain a κ-casein enriched fraction (Post, Arnold, Weiss, & Hinrichs, 2012), whereas the precipitate was reconstituted in ultrapure water to obtain 2.5% casein (w/v), after which NaOH (2 M) was added to pH 7.0, followed by incubation at 4 °C for 6 h. HCl (2 M) was then added to pH 4.6, followed by centrifugation at 4 °C and 10,000×*g* for 15 min, after which the supernatant was incubated at 35 °C for 0.5 h, followed by centrifugation at 10,000×*g* for 15 min to obtain a β-casein enriched fraction (Thienel et al., 2018). The κ- and β-caseins enriched fractions were reconstituted in ultrapure water, and dialyzed against ultrapure water at 4 °C using a tube with a nominal molecular weight cut-off of 7 kDa (Shanghai Green Bird Science and Technology Development Co., Shanghai, China), followed by lyophilization using a BenchTop Pro freeze drier (SP Scientific Co., Stone Ridge, NY, USA) and then mixing (7:3, w/w) to obtain formulated caseins with compositions similar to that of human caseins according to a preliminary experiment involving different mixing ratios. The κ-casein-enriched fraction contained, β-, κ- and α_{s1}-caseins with a ratio of 57:27:16, while the α_{s1}-, α_{s2}-, and κ-caseins were negligible for the β-casein-enriched fraction.

2.3. Formation of casein micelles

The formulated caseins were reconstituted in ultrapure water to obtain a dispersion with 0.8% (w/v) caseins. The formation of casein micelles was done (Table S1) according to the method of Hemar et al. (2020) with modifications. The formulated casein dispersion (10 mL) in a 50 mL jacketed glass beaker was maintained at 37 °C using a MP-501A circulating water bath (Yiheng Technical Co., Ltd., Shanghai, China). Stock solutions of $K_3C_6H_5O_7$ (Cit, 200 μL, 230 mM), $CaCl_2$ (Ca, 3 mL, 40 mM), K_2HPO_4 (Pi, 3 mL, 19 mM) or KCl (K, 1 mL, 300 mM) were added dropwise with continuous magnetic stirring, followed by adjusting the pH to 7.0. The total volume was brought to 20 mL with ultrapure water.

To study the effect of added mineral composition, the mineral stock solutions were added sequentially for each case as follows: Ca; Ca → Pi; Cit → Ca; Cit → Ca → Pi; Cit → Ca → Pi → K. To study the effect of mineral addition order, the mineral stock solutions were added sequentially for each case as follows: Cit → Pi → Ca; Pi → Cit → Ca; Ca →

Cit → Pi; Ca → Pi → Cit; Cit → Ca → Pi; Pi → Ca → Cit. To study the effect of mineral addition cycle, the mineral stock solutions were added using two sequences: Cit → (Ca → Pi) × n, where all Cit was added first and then a 1/n portion of Ca and Pi were added sequentially for n cycles; and (Cit → Ca → Pi) × n, where a 1/n portion of Cit, Ca and Pi were added sequentially for n cycles; n = 1–4.

To study the effect of mineral concentration, different concentrations of Cit (0–690 mM), Ca (0–107 mM) and Pi (0–121 mM) stock solutions were prepared. The mineral stock solutions were added sequentially: (Cit → Ca → Pi) × 3, where the concentrations of the stock solutions of Cit, Ca and Pi were 230, 0–107 and 19 mM for the effect of Ca, 0–690, 40 and 19 mM for the effect of Cit, and 230, 40, 0–121 mM for the effect of Pi, respectively.

Optical absorbance of the casein micelle dispersions in a 5 mm pathlength quartz cuvette was measured at 400 nm using an UV-2700 spectrophotometer (Shimadzu Corp., Kyoto, Japan).

2.4. In vitro gastrointestinal digestion

An *in vitro* infant gastrointestinal digestion was done in the 50 mL jacketed glass beaker at 37 °C, according to the method of Ménard et al. (2018). Enzyme activities for porcine pepsin and pancreatin were measured using hemoglobin (from bovine blood) as the substrates, respectively, following the method of Brodkorb et al. (2019). For gastric digestion, the casein micelle dispersion was mixed (63:37, v/v) with a simulated gastric fluid (724.3 U pepsin/mL gastric fluid, 13 mM KCl, and 94 mM NaCl, pH 5.3), followed by readjusting the pH to 5.3 with 1 M HCl. After gastric digestion, the digesta was adjusted to pH 7.0 with 2 M NaOH, and then mixed (62:38, v/v) with a simulated intestinal fluid (42.1 U trypsin/mL intestinal fluid, 8.2 mM bile, 10 mM KCl, and 249 mM NaCl, pH 6.6). This was readjusted to pH 6.6 with 2 M HCl. Digesta were collected at 1, 3, 6, 10, 20, 30 and 60 min during both the gastric and intestinal digestion. Pepstatin A (7.3 μM) and Pefabloc SC (5.0 mM) were added to stop the pepsinolysis or trypsinolysis, respectively. Digesta without the proteases were the control, which was collected at 0 min. A 2 mL portion of the digesta was placed in a Petri-dish (35 mm in diameter) and photographed using an IXUS 210 digital camera (Canon Inc., Tokyo, Japan).

2.5. Analytical methods

2.5.1. Determination of casein and mineral distribution

The casein micelle dispersions were ultracentrifuged at 150,000×*g* for 1 h at 25 °C using the Optima L-100XP ultracentrifuge. The protein content of the dispersion and its supernatant were measured using a Kjeldahl method (ISO, 2001) with a K1302 apparatus (Sonnen Automated Analysis Instrument Co., Ltd., Shanghai, China) for total and serum caseins, respectively, using a Kjeldahl factor of 6.38. The difference between total and serum caseins was assumed to be the micellar casein. To determine casein composition, the dispersion and its supernatant were mixed (1:1, v/v) with a 0.1 M Bis-Tris-propane buffer (pH 7) containing 8 M urea, 20 mM dithiothreitol and 1.3% (w/v) trisodium citrate, respectively, and filtered through a mixed cellulose ester membrane (0.45 μm nominal pore diameter; Xinya, Inc., Shanghai, China). The filtrate was analyzed using reversed-phase high-performance liquid chromatography (RP-HPLC) according to the method of Liu, Zhang, Wang, et al. (2019). An e2695 Separations Module (Waters Corp., Milford, MA, USA) equipped with a Waters XBridge BEH C18 column (250 × 4.6 mm I.D.) and a Waters 2489 UV/visible detector at 220 nm was used. The percentage of each casein in the serum was calculated using its peak area on the supernatant chromatogram relative to that on the corresponding dispersion chromatogram. Protein compositions of bovine caseins and formulated caseins derived from bovine caseins were determined as above, and the ratios of each casein was calculated using its peak area relative to that of all caseins.

For determination of Ca content, the casein micelle dispersion and its supernatant were digested in nitric-perchloric acid (4:1, v/v) using a MARS Microwave Digestion System (CEM Corp., Matthews, NC, USA), followed by analysis using an iCAP TQ inductively coupled plasma mass spectrometer (Thermo Fisher Scientific, Inc., Bremen, Germany). The difference between total and soluble Ca was assumed to be the colloidal Ca. The molar Ca:casein ratio in micelles was calculated assuming a molecular mass of 23.6 kDa for caseins. For the skim milk and formulated casein dispersion, the concentrations of Ca and potassium were determined as above.

The concentrations of Pi and Cit were determined using the methods of ISO (2018) and Garnsworthy, Masson, Lock, and Mottram (2006), respectively. In brief, human skim milk and formulated casein dispersions were first mixed (1:1, v/v) with 30% (w/v) trichloroacetic acid, and centrifuged at 10,000×*g* for 1 h. The Pi and Cit contents of the supernatants were determined using the iCAP TQ inductively coupled plasma mass spectrometer and the RP-HPLC, respectively.

2.5.2. Dynamic light scattering (DLS)

To determine the particle size distribution of the casein micelle dispersion, DLS was done at 25 °C using a Zetasizer Nano ZS device (Malvern Instruments Ltd., Malvern, UK) following the method of Liu, Zhang, Wang, et al. (2019) with slight modifications. A refractive index of 1.57 for casein particles in solution was set before measurement using a scattering angle of 173° (Liu, Zhang, Yang, et al., 2019).

2.5.3. Determination of micellar hydration

The ultracentrifugal pellet collected in section 2.5.1 was oven-dried at 103 °C for 7 h. The difference in weights before and after drying, expressed as g water/g dry pellet, was assumed to be the micellar hydration.

2.5.4. Small angle X-ray scattering (SAXS)

The internal structure of casein micelles was examined using a SAXSpoint 2.0 device (Anton-Paar GmbH, Graz, Austria) at a radiation wavelength of 1.54 Å, according to the method of Mata, Udabage, and Gilbert (2011). The casein micelle dispersion was lyophilized and the powder loaded into a 2 mm thick sample stage with a drilled rectangle (20 × 4 mm) hole sealed using adhesive tapes on each side. The distance of the sample to the detector was set at 600 mm, and scattering was measured under vacuum for 1 h. The two-dimensional data was converted to one-dimensional data using SAXSanalysis 4.00.046 software (Anton-Paar GmbH). Background scattering was collected from an empty stage, and subtracted from the sample scattering.

2.5.5. Cryo-transmission electron microscopy (Cryo-TEM) and atomic force microscopy (AFM)

Cryo-TEM analysis was done using a Talos F200C cryo-transmission electron microscope (Thermo Fisher Scientific) following the method of Wu et al. (2020). A droplet of the casein micelle dispersion was deposited onto a copper grid, and the excess dispersion was blotted with a filter paper. The grid was dropped into liquid ethane for quench-freezing, and then transferred into liquid nitrogen for storage before observation at an acceleration voltage of 200 kV and imaging at 45,000× magnification.

AFM was done using a Dimension ICON atomic force microscope (Brock Technology Co., Ltd, Billerica, MA, USA) according to the method of Ouanezar, Guyomarc'h, and Bouchoux (2012). A droplet of the casein micelle dispersion was deposited onto a cleaned mica sheet, and then dried in a desiccator. The area of the scanned surface was set as 1 × 1 μm^2. Image processing was done using Nanoscope Analysis 1.9 software (Brock Technology).

2.5.6. Confocal laser scanning microscopy (CLSM)

The gastric digesta (0.1 mL) from *in vitro* digestion (Section 2.4) were labeled using fluorescein isothiocyanate (2 μg/mL), and the solution placed into a glass bottom cell culture dish (Shengyou Biotechnology

Co., Huzhou, Zhejiang, China). Observations were done using a TCS SP8 confocal laser scanning microscope (Leica Microsystems CMS GmbH, Mannheim, Germany) at excitation and emission wavelengths of 488 and 498–532 nm, respectively. Imaging was done using a 10× objective lens.

2.5.7. Sodium dodecyl sulphate-polyacrylamide gel electrophoresis (SDS-PAGE)

SDS-PAGE on gastric *in vitro* digesta (Section 2.4) was done using a Mini-PROTEAN Tetra Cell system (Bio-Rad Laboratories, Inc., Hercules, CA, USA) loaded with a 4% stacking gel and a 13% resolving gel according to the method of Liu, Zhang, Wang, et al. (2019). The digesta was mixed (1:1, v/v) with a 62.5 mM Tris-HCl buffer (pH 6.8) containing 2% (w/v) SDS, 5% (v/v) β-mercaptoethanol and 25% (v/v) glycerol. The mixture was boiled for 3 min, and then a 10 μL sample was loaded in each well. After electrophoresis, the gel was stained using 0.1% (w/v) Coomassie Brilliant Blue R-250 for 4 h, and then destained using 7.5% (v/v) acetic acid and 5% (v/v) methanol until clear bands were visible. Semi-quantitative analysis of the band intensity was done using a ChemiDoc XRS + Imager loaded with an Image Lab™ 3.0 software (Bio-Rad Laboratories).

2.5.8. OPA spectrophotometric assays

Free amino groups in the gastric and intestinal *in vitro* digesta (Section 2.4) were determined according to the method of Wang et al. (2023) using L-leucine as the standard. The sample was mixed (1:1, v/v) with 6.2% trichloroacetic acid, and then centrifuged at 10,000×*g* for 10 min. Supernatant (150 μL) was mixed with 3 mL of 0.08% (w/v) OPA, 3.8% (w/v) $Na_2B_4O_7$, 0.1% (w/v) SDS and 0.09% (w/v) dithiothreitol. After incubation in the dark for 15 min, the absorbance was measured at 340 nm using the spectrophotometer.

2.5.9. High performance size exclusion chromatography (HPSEC)

The molecular weight distribution of peptides in the gastric and intestinal *in vitro* digesta (Section 2.4) was determined using the Waters e2695 Separations Module equipped with a TSK gel G2000SWXL column (300 × 7.8 mm I.D., Tosoh Bioscience LLC, Montgomeryville, PA, USA) and the 2489 UV/visible detector, according to the method of Wang et al. (2020). The sample was mixed (1:1, v/v) with 8 M urea and then filtered through a nylon membrane (0.45 μm pore diameter; Fuji Science & Technology Co., Ltd., Tianjin, China). Filtrate (40 μL) was injected, and eluted using acetonitrile:water:trifluoroacetic acid (400:600:1, v/v/v) at 0.5 mL/min. To estimate the molecular weight, cytochrome C, aprotinin, bacitracin, Gly-Gly-Arg-Try and Gly-Gly-Gly were used as the standards.

2.6. Statistical analysis

Statistical analysis was done using Statistical Analysis System version 8 (SAS Institute, Inc., Cary, NC, USA). One-way analysis of variance with the General Linear Model procedure was done and the difference between means was determined using the Duncan's test at a significance level of 0.05.

3. Results and discussion

3.1. Formulation of caseins and minerals

Protein compositions of bovine caseins and formulated bovine caseins were analyzed by RP-HPLC and were shown in Fig. S2. The ratio of β-, κ- and α_{s1}-caseins in the formulated caseins was 67.8:20.3:11.9 with α_{s2}-casein being absent. This was similar to the composition of caseins in the human skim milk from 10 mothers, i.e., with β-, κ- and α_{s1}-caseins at a ratio of 67.6:20.7:11.7, which was consistent with values of 68–70:18–21:9–12 reported by Hailu et al. (2016) and Yang et al. (2022). The average concentrations of Cit, Ca, Pi and K in the human skim milk from 10 mothers were 2.3, 7.1, 2.8 and 15.0 mM, respectively, which were consistent with the values of 2.2–2.8, 7.3–7.8, 2.2–2.5, and 15.2–16.5 mM reported by Holt and Jenness (1984) and Holt (1993). The assembly of caseins in milk is strongly affected by these ions (Neville, 2005). The concentration of Ca in the formulated casein dispersion was 1.1 mM, and the concentrations of Cit, Pi and K were negligible. Based on the average mineral concentrations of human milk, Cit, Ca, Pi and K were added into formulated casein dispersions to induce the formation of casein micelles.

3.2. Formation of casein micelles

Fig. 1A showed the effect of added mineral compositions on the absorbance of formulated casein dispersions. With only Ca, the absorbance slightly increased compared to the value of 0.18 for the dispersions. With Cit and Ca, the absorbance decreased compared to with Ca only. With Ca and Pi, the absorbance increased strongly. With Cit, Ca and Pi, the absorbance was approximately midway between the two extremes. With Cit, Ca, Pi and K, the absorbance was the same as with Cit, Ca and Pi. The added Ca could bind to casein monomers and small aggregates via ionic bonds, while shielding net-negative charges to reduce electrostatic repulsions, thus inducing formation of primary particles (Pitkowski, Durand, & Nicolai, 2008; Thomar, Durand, Benyahia, & Nicolai, 2012). Without Ca in the dispersions, the added Pi itself did not bind to caseins and was present in serum phase (Thomar, Gonzalez-Jordan, Dittmer, & Nicolai, 2017). Once monomers and small aggregates were induced by Ca to form primary particles, Pi further induced the formation of large colloidal particles, i.e., formed micelles. The added Cit sequestered Ca in serum phase, resulting in lower level of free Ca, which induced the formation of primary and colloidal particles with moderate size (Thomar et al., 2017). Taken together, the formation of micelles relied on the involvement of Cit, Ca and Pi, with their size determined by the amount of Ca bound to caseins.

As shown in Fig. 1B, with Ca added last, the absorbance was lower. With Ca added first, the absorbance was much larger, and slightly decreased when Cit was added first after Ca, compared to when Pi was added first after Ca. With Ca added in the middle, the absorbance was approximately midway between the two extremes. The Pi and Cit first sequestered most of Ca in serum phase when Ca was added last, and then the lower Ca induced the formation of smaller colloidal particles. The Ca added first induced the formation of large primary particles, and then Pi added in middle further induced the formation of larger colloidal particles; whereas Cit added in middle could sequester part of the Ca, resulting in smaller colloidal particles. The Pi added first with the Ca added later was more likely to form complex in serum phase which was not conducive to the formation of colloidal particles (Thomar et al., 2017). These results suggested that the optimal mineral addition order was Cit followed by Ca, and then Pi.

The formation of human casein micelles mainly occurs in the Golgi bodies of mammary epithelial cells, during which caseins and various minerals are continuously transported to the Golgi apparatus (Neville, 2005). This process could be simulated by controlling the mineral addition cycles, which may prevent an excessive concentration of minerals locally from affecting the size of formed micelles. Fig. 1C showed that the absorbances of formed micelle suspensions had a decreasing trend and gradually approached those of human micelles with the increase of mineral addition cycles. Where the addition cycles were done once and twice, the absorbance of the micelles using the addition sequence Cit → Ca → Pi was closer to that of human micelles compared to the addition sequence Ca → Pi. With three cycles, the absorbances of the above two addition sequences became stable and within the range of human micelles. Therefore, the optimal conditions for formation were: minerals addition using the addition sequence Cit → Ca → Pi for three cycles. These conditions were used to prepare micelles for subsequent studies that were similar in size and structure to human micelles.

The concentrations of minerals in human skim milk differ with

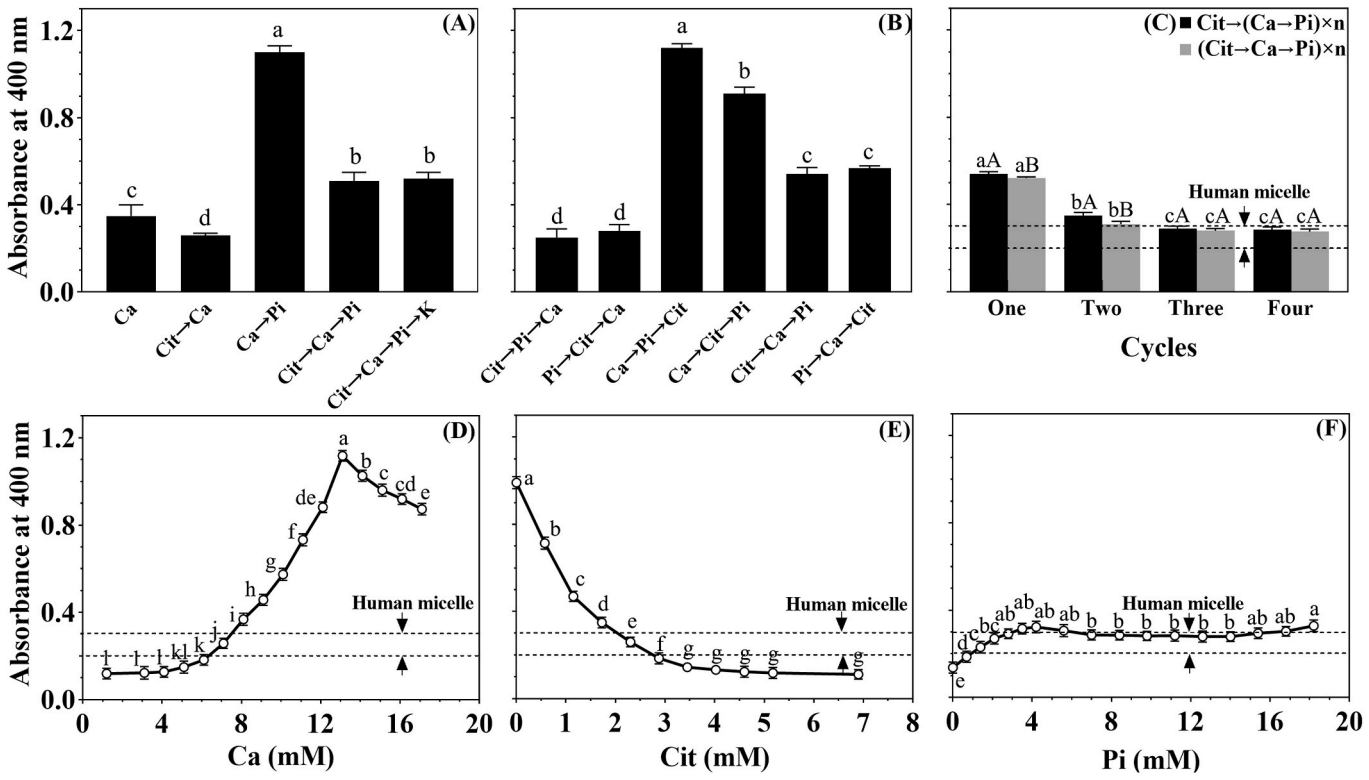

Fig. 1. Optical absorbance of the formulated casein dispersions with different formation conditions: A, added mineral composition (2.3 mM Cit; 7.1 mM Ca; 2.8 mM Pi; 15.0 mM K); B, mineral addition order (2.3 mM Cit; 7.1 mM Ca; 2.8 mM Pi); C, mineral addition cycle (2.3 mM Cit; 7.1 mM Ca; 2.8 mM Pi); D, Ca concentration (1.1–17.1 mM Ca in the presence of 2.3 mM Cit and 2.8 mM Pi); E, Cit concentration (0–7.0 mM Cit in the presence of 7.1 mM Ca and 2.8 mM Pi); F, Pi concentration (0.7–18.2 mM Pi in the presence of 2.3 mM Cit and 7.1 mM Ca). The two dotted lines show the range of optical absorbance of human casein micelle dispersions. Different letters indicate that the data differ significantly among different variables of each formulation condition ($P < 0.05$).

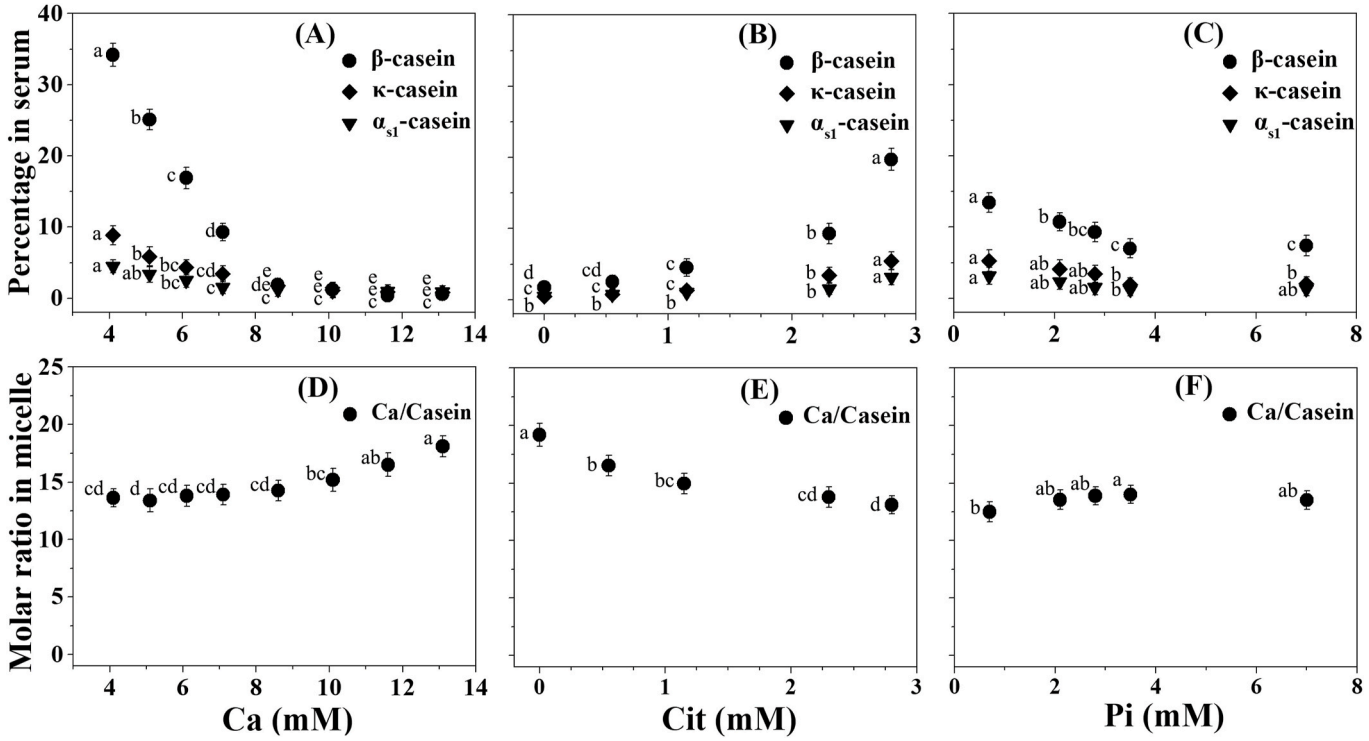

Fig. 2. Percentage of serum caseins (β, κ, α_{s1}) relative to corresponding total protein (A–C) and molar ratio of Ca to caseins (D–F) for casein micelles formed using different conditions: A and D, Ca concentration (4.1–13.1 mM Ca in the presence of 2.3 mM Cit and 2.8 mM Pi); B and E, Cit concentration (0–2.8 mM Cit in the presence of 7.1 mM Ca and 2.8 mM Pi); C and F, Pi concentration (0.7–7.0 mM Pi in the presence of 2.3 mM Cit and 7.1 mM Ca).

geographical region, individual mother's differences, circadian rhythm changes and other factors (Gidrewicz & Fenton, 2014; Neville, 2005). This might be associated with the formation of casein micelles and hence affect the absorbance of human skim milk (Sood et al., 2006). Fig. 1D–F showed the effect of added mineral concentrations on the absorbance of the formulated casein dispersions. For Ca, the absorbance increased slightly between 1.1 and 6.1 mM Ca and then increased gradually from 7.1 to 13.1 mM Ca, followed by a decrease from 14.1 to 17.1 mM Ca. For Cit, the absorbance decreased significantly ($P < 0.05$) with increasing Cit concentration from 0 to 4.0 mM and then remained almost unchanged up to 7.0 mM. For Pi, the absorbance increased gradually between 0 and 4.2 mM and then decreased slightly to 7.0 mM, followed by almost no change to 14.0 mM and then a slight increase between 14.0 and 18.2 mM. When the concentrations of Cit, Ca and Pi were 2.1–2.8, 6.1–7.1 and 1.5–3.0 mM, respectively, the absorbance of the formulated casein dispersions were within the absorbance range of human micelles. Based on Fig. 1D–F, the concentrations of Cit, Ca and Pi corresponding to the absorbance range of human micelles were selected for subsequent studies. Hemar et al. (2020) also reported that formed casein micelles with a size similar to native bovine micelles were obtained by titrating Ca and Pi solutions into a sodium caseinate solution, in which the concentrations of these ions and caseins were the same as native bovine micelles.

3.3. Physicochemical properties of formed casein micelles

3.3.1. Distribution of caseins and Ca

Fig. 2 showed the percentages of serum β-, α_{s1}-and κ-casein relative to the corresponding total caseins and the molar ratio of Ca:micellar casein in formed micelles using different Cit, Ca, and Pi concentrations. With Ca concentration increasing from 4.1 to 8.6 mM, the percentages of serum β-, κ- and α_{s1}-casein decreased from 34 to 1%, from 10 to 1 % and from 5% to 1%, respectively, and the Ca:casein molar ratio in micelles increased slightly from 13.6:1 to 14.2:1. With Ca concentration increasing from 8.6 to 13.1 mM, the percentages of serum caseins remained almost unchanged, and the Ca:casein molar ratio in micelles increased significantly ($P < 0.05$) from 14.2:1 to 18.1:1 (Fig. 2A and D). With Cit concentration increasing from 0 to 2.8 mM, the percentages of serum β-casein increased from 1 to 20%, whereas the percentages of serum κ- and α_{s1}-caseins showed a slight increasing trend, and the Ca:casein molar ratio in micelles decreased from 19:1 to 13:1 (Fig. 2B and E). With Pi concentration increasing from 0.7 to 3.5 mM, the percentages of serum β-casein decreased from 13 to 7%, and the Ca:casein molar ratio in micelles increased from 12:1 to 14:1. With increasing Pi concentration up to 7.0 mM, the serum β-casein percentages increased to 7.4%, and the Ca:casein molar ratio decreased to 13.5:1 (Fig. 2C and F). These results were consistent with the absorbance of the formulated casein dispersions (Fig. 1D–F).

With the average concentration of Cit, Ca and Pi in human milk, the serum β-casein (10%; Fig. 2) was lower than the 18% of human milk (Yang et al., 2022), and the Ca:casein molar ratio in formed micelles (13.9:1; Fig. 2) was higher compared to the 8.8:1 found for human micelles (Yang et al., 2022). The degree of phosphorylation of formulated caseins derived from bovine caseins was higher than that of human caseins, and the higher degree of phosphorylation of caseins allows Ca and caseins associating into micelles more easily (Huppertz, 2013; Yang et al., 2022). The percentage of each casein remained in serum for formed micelles (Fig. 2) was consistent with that for human casein micelles, i.e., β- > κ- > α_{s1}-caseins (Yang et al., 2022). For casein micelles formed using excess Ca (13.1 mM), the caseins and Ca were predominantly associated into micelles, resulting in the Ca:casein molar ratio (18:1) of formed micelles being much higher than human micelles, and closer to the value of 19:1 for bovine micelles (Holt et al., 1984). For casein micelles formed with different Cit levels, the added Cit sequestered Ca, reducing the contents of micellar Ca and micellar caseins. For casein micelles formed with different Pi levels, the added Pi induced the formation of more calcium phosphate nanoclusters (CCP), thus increasing the content of micellar Ca and micellar caseins, whereas excess Pi competed with caseins for Ca, resulting in a decrease of micellar Ca and micellar caseins.

3.3.2. Particle size distribution and micellar hydration

Fig. 3 showed the particle size distribution and micellar hydration of casein micelles formed with different amounts of Cit, Ca, and Pi. With the increase of Ca concentration, particle size distribution generally shifted towards larger sizes (Fig. 3A). When the concentration of Ca increased from 4.1 to 10.1 mM, the particle size increased from 40 to 100 nm and the size distributions were mono-modal; while micellar hydration decreased from 5.9 to 1.9 g water/g dry matter (Fig. 3D). With the increase of Ca concentration from 10.1 to 13.1 mM, the particle size continued to increase but showed a multi-modal pattern with the uniformity decreasing, and micellar hydration remaining unchanged (1.9 g water/g dry matter). With the increasing Cit concentration from 0 to 7.0 mM, particle size decreased from 130 to 60 nm (Fig. 3B) and micellar hydration increased from 2.6 to 3.9 g water/g dry matter (Fig. 3E). With the increase of Pi from 0.7 to 3.5 mM, the particle size increased from 50 to 90 nm (Fig. 3C) and micellar hydration decreased from 5.0 to 3.0 g water/g dry matter (Fig. 3F). When the concentration of Pi further increased to 7.0 mM, particle size decreased to 70 nm and micellar hydration increased to 3.3 g water/g dry matter (Fig. 3C and F). These results agreed with the absorbances of formulated caseins dispersions (Fig. 1D–F).

Using the average concentration of Cit, Ca, and Pi in human milk, the particle size of formed micelles (~78 nm) was within the size range of human micelles (60–80 nm) (Meng et al., 2021) and that micellar hydration (3.2 g water/g dry matter) was close to the value of ~3.4 for human casein micelles (Yang et al., 2022). These micelles also showed a similar loose structure as human micelles. For casein micelles formed with different Ca levels, excess Ca made the particle size distribution and micellar hydration closer to bovine micelles (2.3 g water/g dry matter; 150 nm) and induced the formation of a compact micellar structure. For casein micelles formed with different Cit levels, Cit in the serum phase sequestered Ca, decreasing the contents of micellar Ca and micellar caseins, further decreasing the micellar size and density. For casein micelles formed with different Pi levels, serum Ca and caseins gradually associate into micelles with the induction of Pi, increasing the micellar size and density; whereas excess Pi competed with caseins for Ca, decreasing the contents of micellar Ca and micellar caseins, and further decreasing micellar size and density.

3.3.3. Internal structure and morphology

Fig. 4 showed the SAXS curves of micelles formed with different Cit, Ca, and Pi levels. The SAXS curves of powders showed an inflexion point at ~0.045 $Å^{-1}$ corresponding to the mean interparticle correlation length of CCP nanoclusters distributed within micelles (Liu, Zhang, Yang, et al., 2019). Yang et al. (2022) reported that a mid-Q inflexion was observed in the SAXS curves of human micelle powder. Liu, Zhang, Yang, et al. (2019) also reported that the mid-Q inflexion appeared in the powder SAXS curves of milk protein concentrate containing casein micelles, whereas the mid-Q inflexion was not observed in SAXS curves of milk protein concentrate dispersions. The appearance of the mid-Q inflexion for powder scattering might be attributed to both the enhancement of scattering contrast by replacing water with air in the surrounding matrix and the increased packing density of CCP nanoclusters due to drying (Mata et al., 2011).

For casein micelles formed with different Ca levels, a faint inflexion in the mid-Q was observed when the concentration of Ca was 4.1 mM (Fig. 4A). The mid-Q inflexion showed a slight increase in scattering intensity between 4.1 and 7.1 mM and then strongly increased between 8.1 and 13.1 mM Ca, suggesting the formation of more internal structural features of formed micelles. This corresponded well with the increase in Ca:casein molar ratio in micelles with the increase of Ca

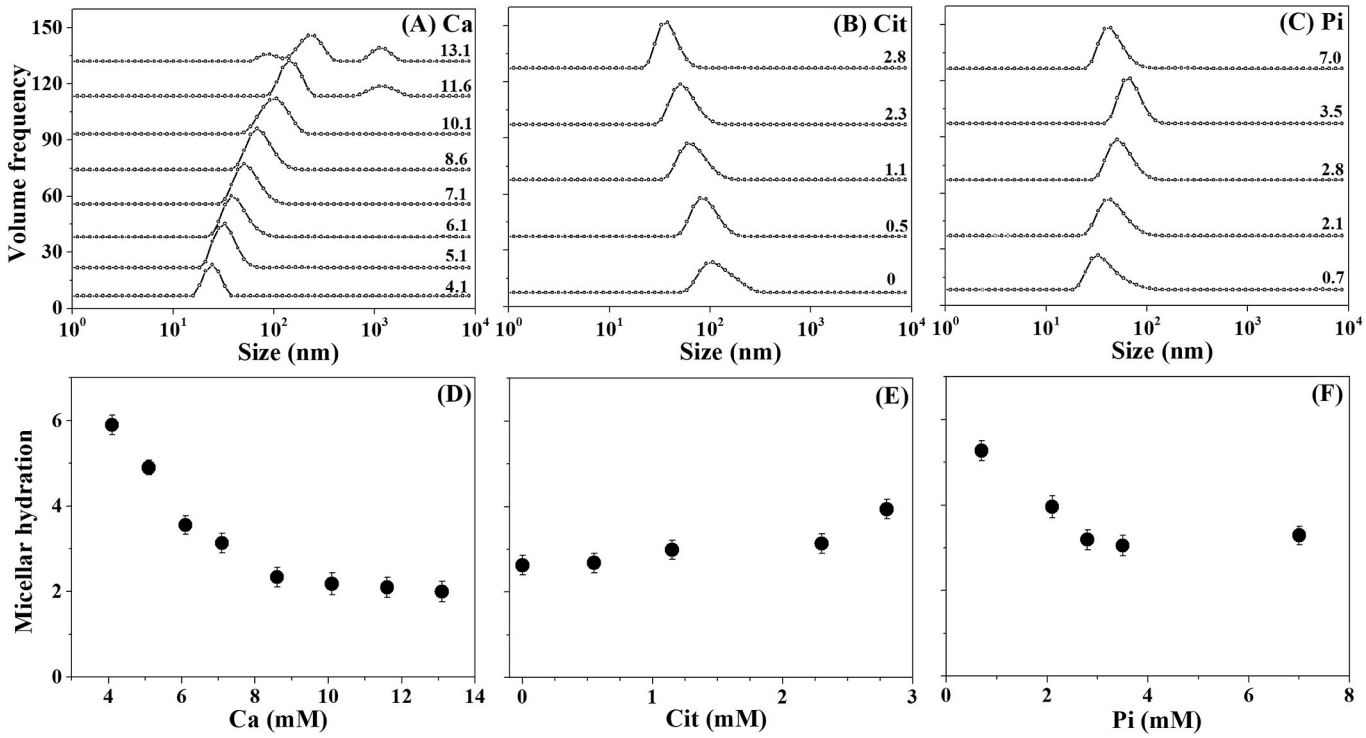

Fig. 3. Particle size distribution (A–C) and micellar hydration (D–F) of casein micelles formed using different conditions: A and D, Ca concentration (4.1–13.1 mM Ca in the presence of 2.3 mM Cit and 2.8 mM Pi); B and E, Cit concentration (0–2.8 mM Cit in the presence of 7.1 mM Ca and 2.8 mM Pi); C and F, Pi concentration (0.7–7.0 mM Pi in the presence of 2.3 mM Cit and 7.1 mM Ca).

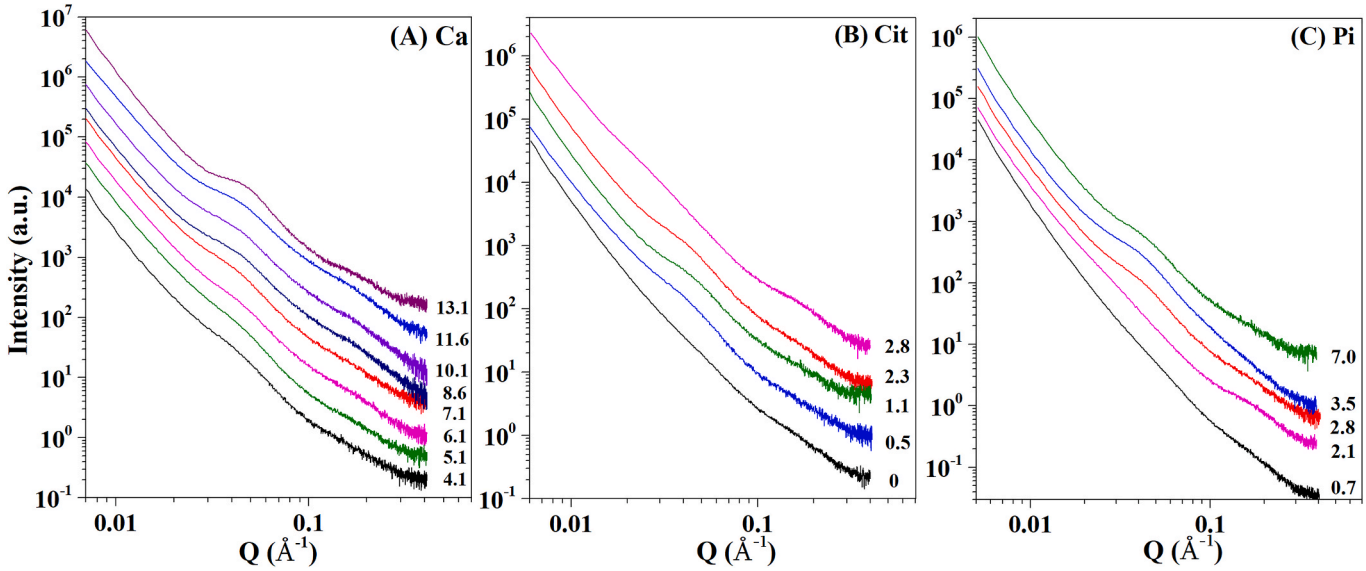

Fig. 4. SAXS profiles of casein micelles formed using different conditions: A, Ca concentration (4.1–13.1 mM Ca in the presence of 2.3 mM Cit and 2.8 mM Pi); B, Cit concentration (0–2.8 mM Cit in the presence of 7.1 mM Ca and 2.8 mM Pi); C, Pi concentration (0.7–7.0 mM Pi in the presence of 2.3 mM Cit and 7.1 mM Ca).

concentration (Fig. 2D). For casein micelles formed with different Cit levels, no inflexion was observed in the mid-Q when Cit was 0 mM (Fig. 4B). The mid-Q inflexion appeared at 0.5 mM Cit and then showed an increase in scattering intensity between 0.5 and 2.3 mM, followed by a disappearance at 2.8 mM. However, the Ca:casein molar ratio in formed micelles decreased with the increase of Cit concentration (Fig. 2E), suggested that a certain amount of Cit was necessary for the formation of micellar internal structure, whereas excess Cit could result in the disappearance of internal structural features.

For casein micelles formed with different Pi levels, no characteristic inflexion was observed in the mid-Q when Pi concentration was 0.7–2.1 mM (Fig. 4C). The mid-Q inflexion appeared at 2.8 mM Pi and then showed an increase in scattering intensity between 2.8 and 3.5 mM, followed by its disappearance at 7.0 mM, which corresponded well with the results of the Ca:casein molar ratio in micelles with increasing Pi concentration (Fig. 2F). These results also suggested that a certain amount of Pi was necessary for the formation of micellar internal structure. Taken together, the micelles formed with the average Cit, Ca, and Pi concentrations of human milk could form an internal structure similar to native human micelles.

Fig. 5 showed the morphology of formed micelles with 7.1 mM Ca (FM-7.1-Ca), human micelles and bovine micelles. Cryo-TEM observations showed that FM-7.1-Ca, human micelles and bovine micelles all have irregular spherules with dark internal structures (Fig. 5A–C), which are similar to the native micellar morphology of bovine and human milk observed by Wu et al. (2020) and Yang et al. (2022) using cryo-TEM. The FM-7.1-Ca was uniformly dispersed with a size similar to human micelles, and much smaller than bovine micelles. Similarly, individual micelles in FM-7.1-Ca, human micelles, and bovine micelles can be observed using AFM (Fig. 5D–F). The micelles in the three types of micelles all showed typical nano roughness and surface irregularities, which were similar to the morphology of native bovine micelles observed by Ouanezar et al. (2012) using AFM. These results were generally consistent with cryo-TEM observations that the size of FM-7.1-Ca were similar to human micelles and much smaller than bovine micelles. These results corresponded with the size distribution of formed micelles shown in Fig. 3A.

In milk, the casein micelles are supramolecular assemblies of caseins and CCP, and are in dynamic equilibrium with the serum phase containing minerals mainly as Ca, Pi and Cit, with the former two being saturated. Ca is the major divalent cation that can induce the aggregation of caseins via ionic bonds, and the major anions competing with caseins for Ca are Pi and Cit, indicating an essential and synergetic role of Ca, Pi and Cit in forming the micelles (Thomar et al., 2017). Ca can bind to Pi and form CCP, which cross-links caseins via their phosphoserine residues. Cit can sequester Ca and hence modulate the amounts of Ca participated directly in cross-linking caseins, thus affecting the formation of micelles (Pitkowski et al., 2008). This is consistent with the assembly process of native micelles in the Golgi of mammary epithelial cells, where caseins and these three minerals are continuously enriched (Neville, 2005). The results of this study also showed that these three minerals and their addition approaches and concentrations were crucial in forming micelles similar to human micelles.

Huppertz et al. (2017) suggested that casein micelles were composed of non-spherical particles similar to primary particles formed by Ca induced ionic bonds, i.e., caseins were polymerized into primary particles, which then associated into a three-dimensional network using the cross-linking of the particles through CCP. The results of this study were consistent with the above micellar structure. Due to the binding constant of Cit to Ca being higher than that of Pi (Philippe, Le Graët, & Gaucheron, 2005), part of the Ca was first sequestered by Cit and remained in the serum phase. An amount of Ca induced casein aggregation to form primary particles and the remaining Ca was bound to Pi to promote the formation of CCP (Khan, Hemar, Li, Yang, & De Leon-Rodriguez, 2023). Primary particles bound with the CCP via the phosphorylation centers, and also bound to the caseins on the surface of adjacent CCP through hydrophobic interactions, forming the colloidal particles, i.e., formed micelles. The micellar surface was predominantly covered by κ-casein, which maintained micellar stability through electrostatic repulsion and steric hindrance effects (Huppertz et al., 2017). Holt, Wahlgren, and Drakenberg (1996) added Cit, Ca, and Pi into β-casein phosphopeptide solutions at pH 5.5, and slowly increased the pH to 6.7 through ammonia production via urease-induced urea hydrolysis to obtain CCP covered by casein phosphopeptides, showing that the interaction between the caseins and CCP via the phosphorylation centers of the caseins, further participating in the formation of micelles.

3.4. Gastrointestinal digestibility of formed casein micelles

3.4.1. Gastric coagulation and proteolysis

Three micelles (FM-4.1-Ca, FM-7.1-Ca, FM-10.1-Ca) were formed with different total Ca concentrations (4.1, 7.1, 10.1 mM) in the presence of 2.3 mM Cit and 2.8 mM Pi. The morphology and microstructure of the flocs formed during the *in vitro* gastric digestion of formed micelles, human and bovine micelles with infant gastric conditions were shown in Fig. 6. For FM-4.1-Ca micelles, small and loose flocs were

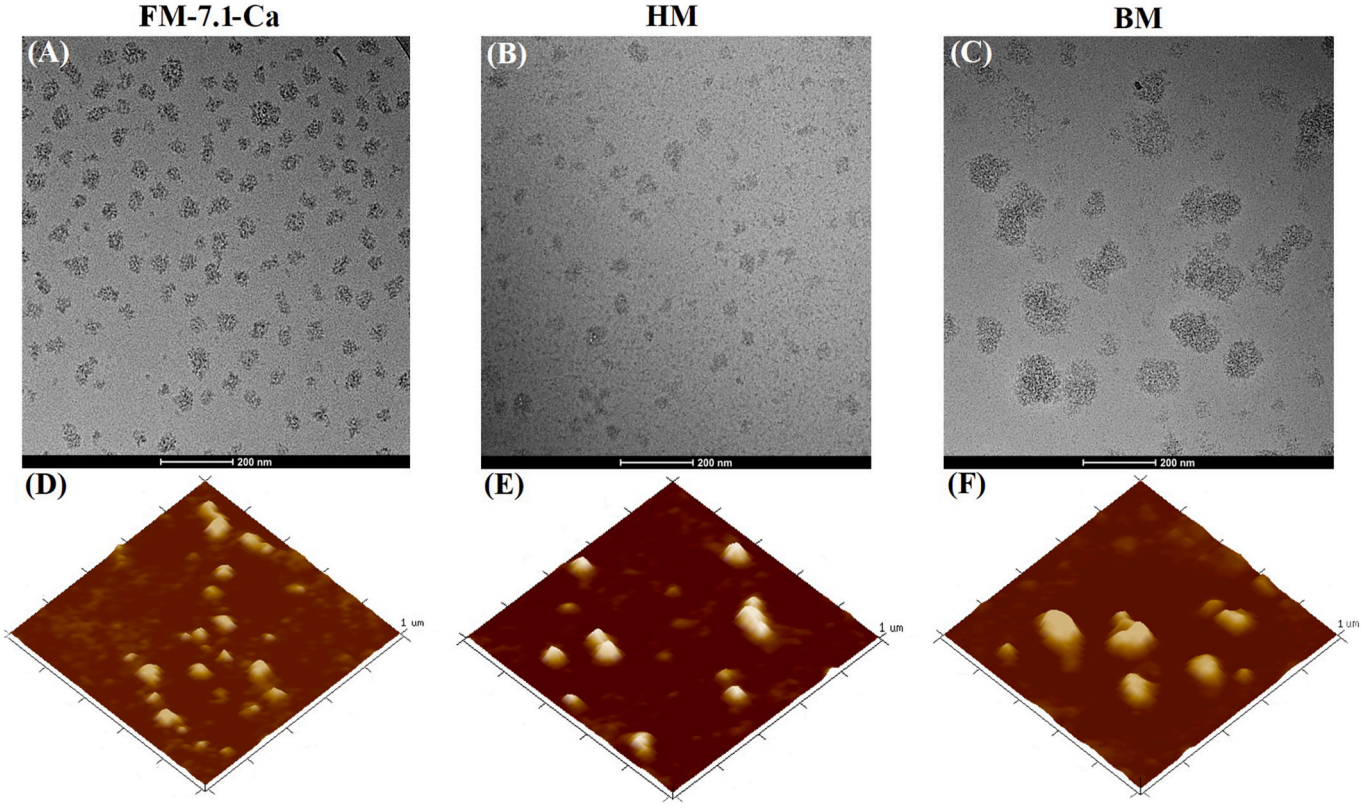

Fig. 5. Cryo-TEM (top) and AFM (bottom) micrographs of casein micelles formed with 7.1 mM Ca in the presence of 2.3 mM Cit and 2.8 mM Pi (A and D), human casein micelles (B and E) and bovine casein micelles (C and F).

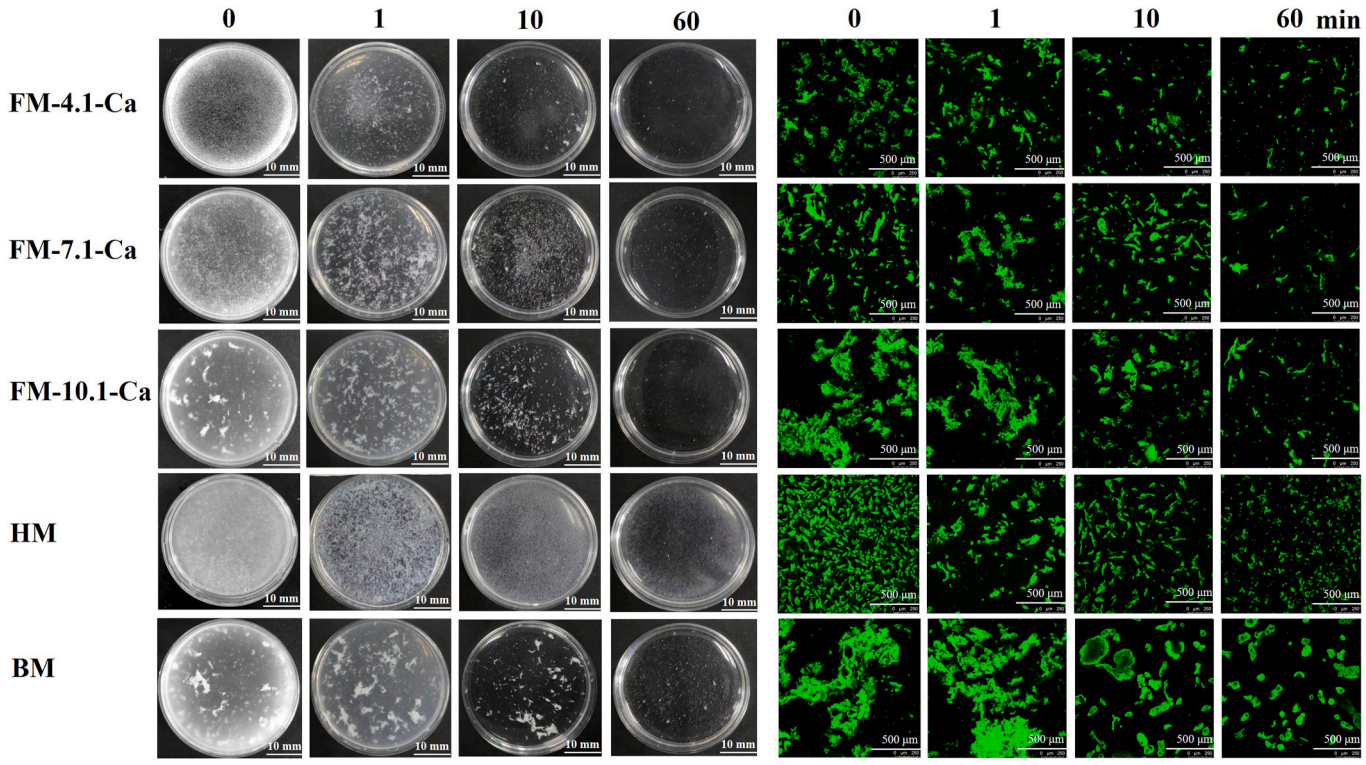

Fig. 6. Visual appearance (left) and CLSM micrographs (right) of the *in vitro* infant gastric digesta of casein micelles formed with 4.1, 7.1 or 10.1 mM Ca in the presence of 2.3 mM Cit and 2.8 mM Pi, human casein micelles and bovine casein micelles.

formed upon decreasing the pH to 5.3 at 0 min, and then slightly larger fragmented flocs were formed after adding pepsin (1 min), followed by a gradual decrease in size with increasing time. The gastric flocs of formed micelles grew markedly in size with the increase of total Ca concentration, and the flocs of FM-7.1-Ca were closer to that of human micelles, and smaller than bovine micelles.

The degradation of caseins during the *in vitro* gastric digestion of different micelles was shown in Fig. 7. For the three formed micelles, intact caseins bands disappeared at 20, 30 and 60 min of gastric digestion with the increase of total Ca concentration, respectively, and

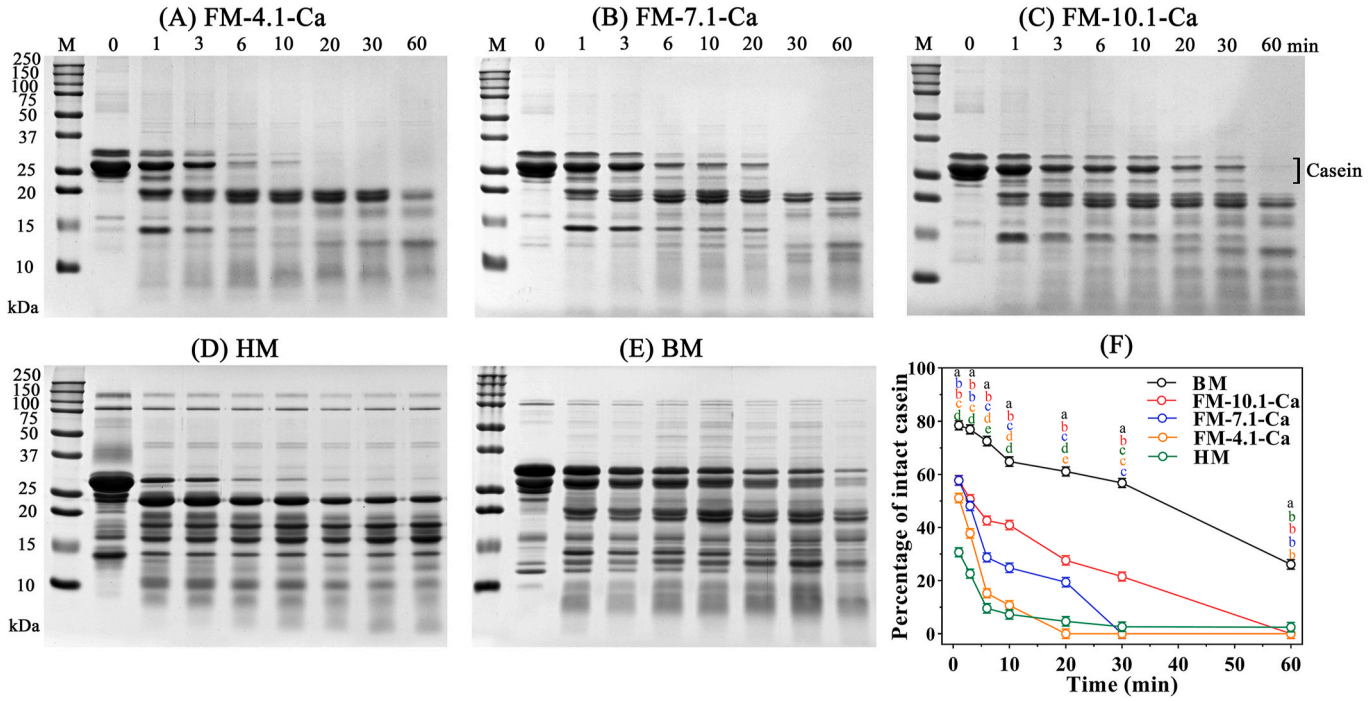

Fig. 7. SDS-PAGE patterns (A–E) and percentage of remaining intact caseins (F) of the *in vitro* infant gastric digesta of casein micelles formed with 4.1 (A), 7.1 (B) or 10.1 (C) mM Ca, human casein micelles (D) and bovine casein micelles (E). M, protein marker. Different letters indicate that the data differ significantly among different micelles at a same digestion time ($P < 0.05$).

peptide fragments were dominated by the 20 kDa fractions. For human micelles, the intact caseins were rapidly hydrolyzed by pepsin at 3–10 min, and the peptide fragments were dominated by the 15–20 kDa fractions. For bovine micelles, the percentage of intact caseins decreased steadily with time and remained at 26% at 60 min, and the intact caseins bands were estimated by linear extrapolation to disappear at ~90 min, indicating a higher resistance to gastric digestion.

The formation of free amino groups during the *in vitro* gastric digestion of different micelles was shown in Fig. 8A. For all samples, the amounts of free amino groups increased sharply within the initial 30 min, followed by a gradual increase until the end, indicating an increasing level of proteolysis. For the three formed micelle samples, the amounts of free amino groups decreased with the increase of total Ca concentration, much greater than bovine micelles, and the free amino groups amounts of FM-4.1-Ca and FM-7.1-Ca were closer to that of human micelles. The above results corresponded to that of the caseins degradation (Fig. 7).

The molecular weight distribution of peptides formed at 60 min of *in vitro* gastric digestion of different micelles was shown in Fig. 8B. For the three formed micelles, with the increase in total Ca, the abundance of the 5–10 and >10 kDa fractions increased gradually with a concomitant decrease in the abundance of 1–5 and <1 kDa fractions. The abundance of the <1 kDa fraction generally was in the order of bovine micelles < FM-10.1-Ca < FM-7.1-Ca < FM-4.1-Ca < human micelles (Fig. 8). Although the abundance of >10 kDa fractions in human micelles was higher compared to formed micelles, the abundance of <1 kDa fractions was the largest, consistent with the result of the electrophoresis pattern of human micelles (Fig. 7D).

The gastric flocs and their proteolysis during the digestion of casein micelles were largely affected by their protein composition and total Ca concentration. Zhang et al. (2022) compared the digestibility of infant formula powders containing different casein components with the *in vitro* gastric digestion of infants, and found that with the increase of β-casein in casein components, the gastric floc particles of infant formula gradually decreased and the casein degradation rate gradually increased. Wang et al. (2023) reported that with the infant gastric conditions, looser and more fragmented clusters and hence a faster casein degradation were observed for bovine micelles with 40% decalcification, compared to those without decalcification. Zou et al. (2022) reported that with the infant gastric conditions, bovine micelles showed dense and hard clusters during digestion, while human milk showed no obvious protein aggregation and were easier to digest and hydrolyze during the gastrointestinal digestion. This is partly due to the lower content of Ca and the dominance of β-casein in human micelles (Yang et al., 2022). Upon gastric digestion of casein micelles, the decrease in pH induced the solubilization of colloidal Ca and the collapse of the κ-casein hairy layers, and subsequently the proteolysis by pepsin led to the removal of the κ-casein hairy layers, thus reducing the electrostatic and steric repulsions between micelles (Huppertz & Chia, 2021). The removal of the κ-casein hairy layer also exposed the Ca-sensitive caseins buried within micelles, thus further promoting the occurrence of inter-micellar Ca-bridging (Huppertz & Chia, 2021). These multiple effects contributed to the formation of larger and denser flocs during the gastric digestion of bovine micelles. These larger and denser flocs decreased the accessibility of pepsin to the casein peptide bonds and reduced the rate of gastric proteolysis (Wang et al., 2023).

The three samples containing formed micelles were consistent with human micelles in terms of casein composition. The increased total Ca concentration of the formed micelles led to the formation of larger and denser flocs, and further led to both the lower rate of casein degradation and the lower level of gastric proteolysis (Figs. 7 and 8). For FM-7.1-Ca, the protein composition and total Ca concentration were consistent with that of the human micelles, resulting in gastric flocs and a level of proteolysis closer to human micelles. Meanwhile, the total Ca concentration and the β-casein content in FM-7.1-Ca were much lower and higher than in bovine micelles, respectively, leading to smaller flocs of FM-7.1-Ca than bovine micelles and a casein degradation rate higher than bovine micelles. However, the rate of casein degradation of FM-7.1-Ca was still lower than human micelles, which may be due to the degree of phosphorylation of caseins from cow milk being higher compared to human caseins. Previous studies have reported that with the *in vitro* gastrointestinal digestion conditions of infants, the increase of the degree dephosphorylation of β-caseins, the looser gastric flocs were formed and gastrointestinal digestibility increased (Liu, Zhang, Wang, et al., 2019).

3.4.2. Intestinal proteolysis

The formation of free amino groups during the *in vitro* intestinal digestion of the different micelles was shown in Fig. 9A. For all micelles, compared to the end of gastric digestion, the amounts of free amino groups increased sharply within the initial 30 min, followed by a gradual increase. The amount of free amino groups generally was in the order of bovine micelles < FM-10.1-Ca < FM-7.1-Ca < FM-4.1-Ca < human micelles during the initial 30 min of digestion, while no significant ($P >$

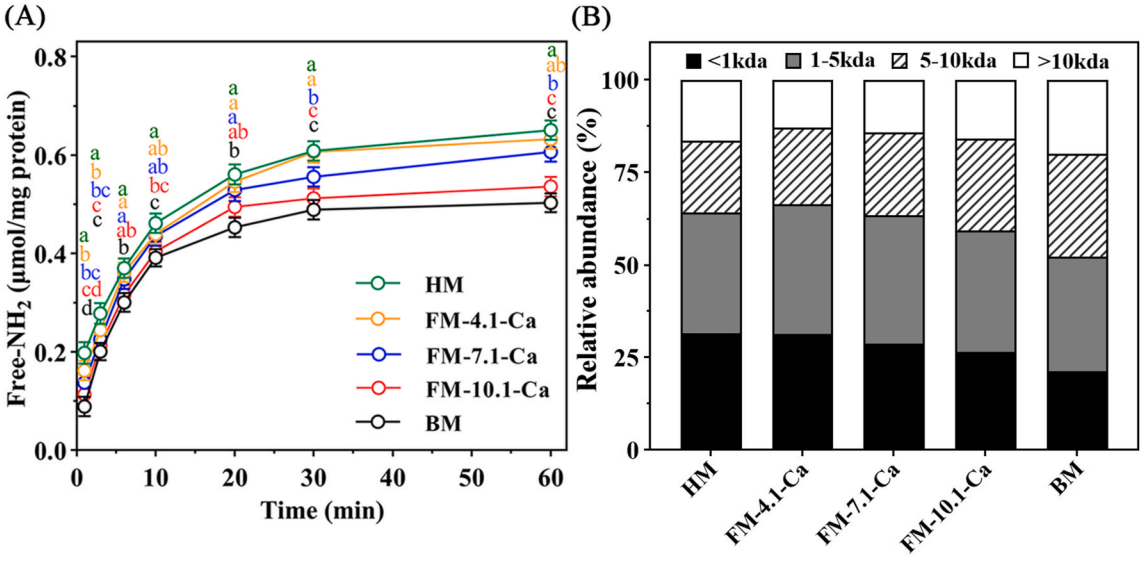

Fig. 8. Amounts of free amino groups (A) and molecular weight distribution of peptides (B) in the *in vitro* infant gastric digesta of casein micelles formed with 4.1, 7.1 or 10.1 mM Ca in the presence of 2.3 mM Cit and 2.8 mM Pi, human casein micelles and bovine casein micelles.

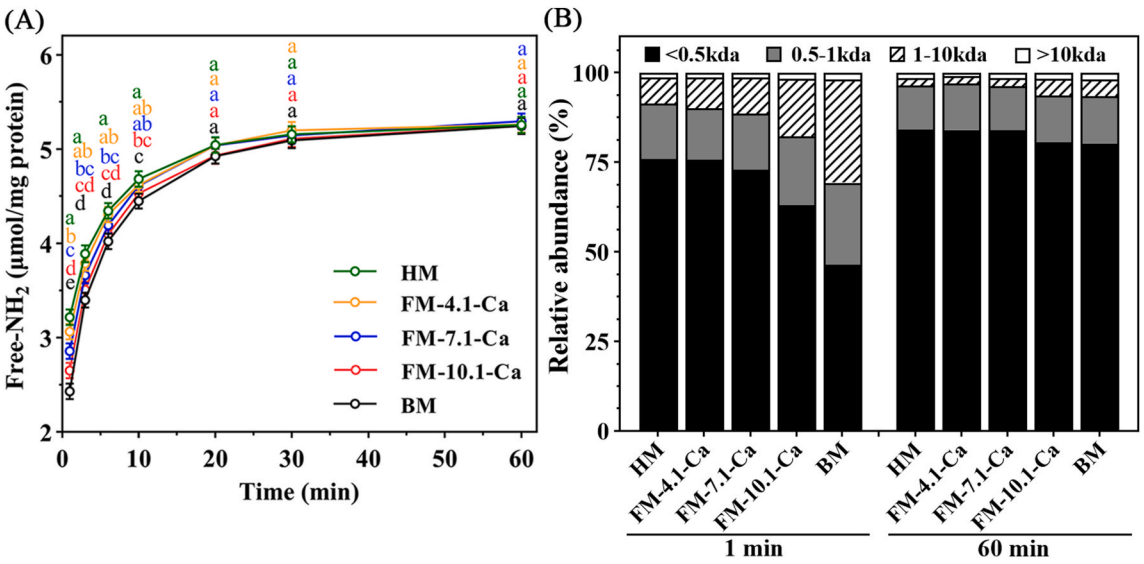

Fig. 9. Amount of free amino groups (A) and molecular weight distribution of peptides (B) in the *in vitro* infant intestinal digesta of casein micelles formed with 4.1, 7.1 or 10.1 mM Ca in the presence of 2.3 mM Cit and 2.8 mM Pi, human casein micelles and bovine casein micelles.

0.05) differences were observed among different micelles at the end of digestion (Fig. 9A). The molecular weight distribution of peptides released in the *in vitro* intestinal digesta was shown in Fig. 9B. For all micelles, compared to the end of gastric digestion, the abundance of the >0.5 kDa fraction decreased gradually with a concomitant increase in the abundance of the <0.5 kDa fraction during digestion (Fig. 9B). The abundance of the <0.5 kDa fraction generally increased in the order of bovine micelles, FM-10.1-Ca, FM-7.1-Ca, FM-4.1-Ca and human micelles at 1 min of digestion. The abundance of the >0.5 kDa fraction for FM-7.1-Ca, FM-4.1-Ca and human micelles was slightly lower compared to FM-10.1-Ca and bovine micelles at 60 min of digestion (Fig. 9B).

Upon intestinal digestion, the increased pH induces an increase in inter-molecular electrostatic repulsions and the concomitant solubilization of the digesta, leading to an increased accessibility of trypsin to peptide bonds and hence more rapid proteolysis (Halabi et al., 2022). With infant intestinal conditions, due to the low pancreatic enzyme addition level, the differences in proteolysis among formed micelles, human micelles and bovine micelles continued to be observed over the first 30 min of the digestion (Fig. 9A and B), further showing that the digestibility of formed micelles was closer to that of human micelles, and higher than bovine micelles. Wang et al. (2023) also reported that for bovine micelles with different degrees of decalcification, the differences in the level of proteolysis obtained after gastric digestion continued to be observed within the initial 30 min of intestinal digestion, and no marked differences were observed in the level of proteolysis at the end of digestion. The accumulation of peptides generally agreed with the formation of free amino groups, i.e., the differences in molecular weight distribution of peptides among different micelles obtained after gastric digestion decreased with time and almost disappeared at the end of digestion, confirming the high efficiency of intestinal proteases.

4. Conclusions

To simulate human micelles, caseins fractionated from bovine caseins were formulated based on the component of human casein, and then Cit, Ca, and Pi were added to formulated casein dispersions to obtain formed casein micelles. The ratio of β-, κ- and α_{s1}-casein in formulated casein dispersions were 68:20:12. The optimal conditions of formation were mineral addition in the order of Cit → Ca → Pi, using three cycles. Optical absorbances showed that the optimal concentrations of Cit, Ca and Pi in formed micelles simulating human micelles were 2.1–2.8, 6.1–7.1 and 1.5–3.0 mM, respectively. FM-7.1-Ca were similar to human casein micelle in particle size, micellar hydration, internal structure and morphology, while the Ca:casein molar ratio in these micelles was higher than human micelles. The microscopic and macroscopic flocs, caseins degradation, free amino groups and molecular weight distribution of peptides showed that gastrointestinal digestibility decreased in the order of human micelles, FM-4.1-Ca, FM-7.1-Ca, FM-10.1-Ca and bovine micelles. The gastric flocs of FM-7.1-Ca was smaller, and formation of free amino groups and small peptides were close to that of human micelles, but the rate of casein degradation of FM-7.1-Ca was still lower than human micelles. The differences in the distribution of caseins and Ca and in the casein degradation rate were probably due to the degree of phosphorylation of caseins from bovine milk being higher than human milk caseins. This study highlighted the important role of formed micelles in simulating human casein components, micellar structure and improving the gastrointestinal digestibility. In turn, formed micelles could be potentially applied in the manufacture of infant formula with improved digestibility.

CRediT authorship contribution statement

Tingting Yang: Investigation, Methodology, Writing-original draft. Dasong Liu: Conceptualization, Writing - review & editing. Jun Tang: Methodology, Writing - review & editing. Xiumei Tao: Methodology, Writing - review & editing. Jielong Zhang: Methodology, Writing - review & editing. Xiaoming Liu: Methodology, Writing - review & editing. Thom Huppertz: Methodology, Writing - review & editing. Joe M. Regenstein: Methodology, Writing - review & editing. Peng Zhou: Conceptualization, Supervision, Funding acquisition.

Declaration of competing interest

The authors declare that they have no known competing financial interests or personal relationships that could have appeared to influence the work reported in this paper.

Data availability

The authors do not have permission to share data.

Acknowledgements

This study was partly supported by the National Key R&D Program of

China (2023YFF11034, 2022YFD2101504), the National Natural Science Foundation of China (31901613), the National High-end Foreign Expert Project of China (G2022144006L), the Fundamental Research Funds for the Central Universities (JUSRP121077), and the Collaborative Innovation Centre of Food Safety and Quality Control of Jiangsu Province.

Appendix A. Supplementary data

Supplementary data to this article can be found online at https://doi.org/10.1016/j.foodhyd.2023.109610.

References

Berton, A., Rouvellac, S., Robert, B., Rousseau, F., Lopez, C., & Crenon, I. (2012). Effect of the size and interface composition of milk fat globules on their *in vitro* digestion by the human pancreatic lipase: Native versus homogenized milk fat globules. *Food Hydrocolloids, 29*, 123–134.

Brodkorb, A., Egger, L., Alminger, M., Alvito, P., Assunção, R., Ballance, S., Bohn, T., Bourlieu-Lacanal, C., Boutrou, R., Carrière, F., Clemente, A., Corredig, M., Dupont, D., Dufour, C., Edwards, C., Golding, M., Karakaya, S., Kirkhus, B., Le Feunteun, S., … & Recio, I. (2019). INFOGEST static *in vitro* simulation of gastrointestinal food digestion. *Nature Protocols, 14*, 991–1014.

Garnsworthy, P. C., Masson, L. L., Lock, A. L., & Mottram, T. T. (2006). Variation of milk citrate with stage of lactation and *de novo* fatty acid synthesis in dairy cows. *Journal of Dairy Science, 89*, 1604–1612.

Gidrewicz, D. A., & Fenton, T. R. (2014). A systematic review and meta-analysis of the nutrient content of preterm and term breast milk. *BMC Pediatrics, 14*, 1–14.

Hailu, Y., Hansen, E. B., Seifu, E., Eshetu, M., Ipsen, R., & Kappeler, S. (2016). Functional and technological properties of camel milk proteins: A review. *Journal of Dairy Research, 83*, 422–429.

Halabi, A., Croguennec, T., Ménard, O., Briard-Bion, V., Jardin, J., Gouar, Y. L., Hennetier, M., Bouhallab, S., Dupont, D., & Deglaire, A. (2022). Protein structure in model infant milk formulas impacts their kinetics of hydrolysis under *in vitro* dynamic digestion. *Food Hydrocolloids, 126*, 107368.

Hemar, Y., Xu, C., Wu, S. N., & Ashokkumar, M. (2020). Size reduction of "reformed casein micelles" by high-power ultrasound and high hydrostatic pressure. *Ultrasonics Sonochemistry, 63*, Article 104929.

Holt, C. (1993). Interrelationships of the concentrations of some ionic constituents of human milk and comparison with cow and goat milks. *Comparative Biochemistry & Physiology, 104*, 35–41.

Holt, C., & Jenness, R. (1984). Interrelationships of constituents and partition of salts in milk samples from eight species. *Comparative Biochemistry and Physiology Part A: Physiology, 77*, 275–282.

Holt, C., Wahlgren, N. M., & Drakenberg, T. (1996). Ability of a β-casein phosphopeptide to modulate the precipitation of calcium phosphate by forming amorphous dicalcium phosphate nanoclusters. *Biochemical Journal, 314*, 1035–1039.

Huang, J. L., Zhang, L. N., Lan, H. L., & Zhou, P. (2022). How to adjust α-lactalbumin and β-casein ratio in milk protein formula to give a similar digestion pattern to human milk? *Journal of Food Composition and Analysis, 110*, Article 104536.

Huppertz, T., & Chia, L. W. (2021). Milk protein coagulation under gastric conditions: A review. *International Dairy Journal, 113*, Article 104882.

Huppertz, T., Gazi, I., Luyten, H., Nieuwenhuijse, H., Alting, A., & Schokker, E. (2017). Hydration of casein micelles and caseinates: Implications for casein micelle structure. *International Dairy Journal, 74*, 1–11.

Huppertz, T., & Timmer, C. (2020). Salt equilibria in nutritional formulae for infants and young children. *International Dairy Journal, 110*, Article 104805.

ISO. (2001). *Milk - determination of nitrogen content - Part 5: Determination of protein-nitrogen content*. Geneva, Switzerland: International Standardisation Organisation. *ISO 8968-5*.

ISO. (2018). *Milk, milk products, infant formula and adult nutritionals - determination of minerals and trace elements - inductively coupled plasma mass spectrometry (ICP-MS) method*. Geneva, Switzerland: International Standardisation Organisation. *ISO 21424-11*.

Khan, M. A., Hemar, Y., Li, J. C., Yang, Z., & De Leon-Rodriguez, L. M. (2023). Fabrication, characterization, and potential applications of re-assembled casein micelles. *Critical Reviews in Food Science and Nutrition*. https://doi.org/10.1080/10408398.2023.2193846

Li-Chan, E., & Nakai, S. (1988). Rennin modification of bovine casein to simulate human casein composition: Effect on acid clotting and hydrolysis by pepsin. *Canadian Institute of Food Science and Technology Journal, 21*, 200–208.

Liu, D. S., Zhang, J., Wang, L. L., Yang, T. Y., Liu, X. M., Hemar, Y., Regenstein, J. M., & Zhou, P. (2019). Membrane-based fractionation, enzymatic dephosphorylation, and gastrointestinal digestibility of β-casein enriched serum protein ingredients. *Food Hydrocolloids, 88*, 1–12.

Liu, D. S., Zhang, J., Yang, T. Y., Liu, X. M., Hemar, Y., Regenstein, J. M., & Zhou, P. (2019). Effects of skim milk pre-acidification and retentate pH-restoration on spray-drying performance, physico-chemical and functional properties of milk protein concentrates. *Food Chemistry, 272*, 539–548.

Mata, J. P., Udabage, P., & Gilbert, E. P. (2011). Structure of casein micelles in milk protein concentrate powders via small angle X-ray scattering. *Soft Matter, 7*, 3837–3843.

Ménard, O., Bourlieu, C., De Oliveira, S. C., Dellarosa, N., Laghi, L., Carrière, F., Capozzi, F., Dupont, D., & Deglaire, A. (2018). A first step towards a consensus static *in vitro* model for simulating full-term infant digestion. *Food Chemistry, 240*, 338–345.

Meng, F., Uniacke-Lowe, T., Ryan, A. C., & Kelly, A. L. (2021). The composition and physico-chemical properties of human milk: A review. *Trends in Food Science & Technology, 112*, 608–621.

Neville, M. C. (2005). Calcium secretion into milk. *Journal of Mammary Gland Biology and Neoplasia, 10*, 119–128.

Ouanezar, M., Guyomarc'h, F., & Bouchoux, A. (2012). AFM imaging of milk casein micelles: Evidence for structural rearrangement upon acidification. *Langmuir, 28*, 4915–4919.

Philippe, M., Le Graët, Y., & Gaucheron, F. (2005). The effects of different cations on the physicochemical characteristics of casein micelles. *Food Chemistry, 90*, 673–683.

Pitkowski, A., Nicolai, T., & Durand, D. (2008). Scattering and turbidity study of the dissociation of casein by calcium chelation. *Biomacromolecules, 9*, 369–375.

Post, A. E., Arnold, B., Weiss, J., & Hinrichs, J. (2012). Effect of temperature and pH on the solubility of caseins: Environmental influences on the dissociation of αs-and β-casein. *Journal of Dairy Science, 95*, 1603–1616.

Roy, D., Ye, A. Q., Moughan, P. J., & Singh, H. (2020). Composition, structure, and digestive dynamics of milk from different species - a review. *Frontiers in Nutrition, 7*, Article 577759.

Sood, S. M., Lekic, T., Jhawar, H., Farrell, H. M., Jr., & Slattery, C. W. (2006). Reconstituted micelle formation using reduced, carboxymethylated bovine κ-casein and human β-casein. *The Protein Journal, 25*, 352–360.

Thienel, K. J. F., Holder, A., Schubert, T., Boom, R. M., Hinrichs, J., & Atamer, Z. (2018). Fractionation of milk proteins on pilot scale with particular focus on β-casein. *International Dairy Journal, 79*, 73–77.

Thomar, P., Durand, D., Benyahia, L., & Nicolai, T. (2012). Slow dynamics and structure in jammed milk protein suspensions. *Faraday Discussions, 158*, 325–339.

Thomar, P., Gonzalez-Jordan, A., Dittmer, J., & Nicolai, T. (2017). Effect of orthophosphate and calcium on the self-assembly of concentrated sodium caseinate solutions. *International Dairy Journal, 64*, 1–8.

Wang, K. Y., Liu, D. S., Tao, X. M., Zhang, J., Huppertz, T., Regenstein, J. M., Liu, X. M., & Zhou, P. (2023). Decalcification strongly affects *in vitro* gastrointestinal digestion of bovine casein micelles under infant, adult and elderly conditions. *Food Hydrocolloids, 139*, 108515.

Wu, S. N., Li, G. T., Xue, Y., Ashokkumar, M., Zhao, H. B., Liu, D. S., Zhou, P., Sun, Y., & Hemar, Y. (2020). Solubilisation of micellar casein powders by high-power ultrasound. *Ultrasonics Sonochemistry, 67*, 105131.

Yang, T. T., Liu, D. S., & Zhou, P. (2022). Temperature-dependent dissociation of human micellar β-casein: Implications of its phosphorylation degrees and casein micelle structures. *Food Chemistry, 376*, Article 131935.

Zhang, J. P., Du, X. Y., Jiang, S. L., Xie, Q. G., Mu, G. Q., & Wu, X. M. (2022). Formulation of infant formula with different casein fractions and their effects on physical properties and digestion characteristics. *Food & Function, 13*, 769–780.

Zou, Z. Z., Duley, J. A., Cowley, D. M., Reed, S., Arachchige, B. J., Koorts, P., Shaw, P. N., & Bansal, N. (2022). Digestibility of proteins in camel milk in comparison to bovine and human milk using an *in vitro* infant gastrointestinal digestion system. *Food Chemistry, 374*, 131704.